



Quad element MIMO antenna for LTE/5G (sub-6 GHz) applications

Ajit Kumar Singh ^a, Santosh Kumar Mahto^a and Rashmi Sinha ^b

^aIndian Institute of Information Technology, Ranchi, India; ^bNational Institute of Technology, Jamshedpur, India

ABSTRACT

A quad-element multiple-input-multiple-output (MIMO) antenna with fractional bandwidth (FBW) of 52.42% (3.35–5.73 GHz) is proposed for LTE, WLAN (4.9/5 GHz), and 5G (sub-6 GHz) applications. The bandwidth is improved by introducing a tapered feed line and rectangular stubs in the partial ground plane. The maximum isolation of the proposed MIMO antenna is 27 dB. The diversity performance characteristics of the proposed antenna are studied in terms of the envelope correlation coefficient (ECC), diversity gain (DG), mean effective gain (MEG), total active reflection coefficient (TARC), isolation between the ports, and channel capacity loss (CCL) and the values obtained are 0.003, 9.98 dB, ± 3 dB, -4 dB, -10 dB, and 0.10 bits/s/Hz respectively. A model of the proposed antenna is fabricated on the FR-4 substrate having a dielectric constant of 4.4 and a loss tangent of 0.02 with an electrical dimension of $0.45\lambda_0 \times 0.45\lambda_0$. The measured results demonstrate a decent likeness to simulated ones in the entire operating frequency range.

ARTICLE HISTORY

Received 29 September 2021
Accepted 7 May 2022

KEYWORDS

5G; tapered fed; partial ground plane; MIMO; mean effective gain; isolation

1. Introduction

The current scenario for mobile communication is to achieve a higher data rate, capacity, low latency, and high resolution. The fifth-generation (5G) mobile communication has been deployed around the world to fulfill the above advantage [1,2]. It has been shown [3,4] that to improve the information throughput in a multipath environment for 5G operations, the MIMO antenna system should be adopted. MIMO antenna systems should have a minimal inter-element distance, low correlation values, and better isolation between inter elements [5]. The primary advantage of adopting an MIMO network over a normal one is that it can enhance wireless connection capacity while consuming less spectrum. The system's link dependability and data rate can be enhanced by increasing the number of antennas on the transmitter/receiver, which results in more signal routes and thus higher performance. Hence MIMO techniques become very vital for wireless communication systems which are suffering from frequency constraints [6,7].

MIMO systems include more antenna elements, a smaller antenna element size is advantageous for establishing a compact design while maintaining acceptable isolation

between elements. Many four-element MIMO antennas have been proposed utilising various approaches for a variety of wireless applications. A four-port MIMO antenna system with a frequency range of 3.2–5.75 GHz has been proposed for use in 5G new radio (NR) sub-6 GHz WLAN applications [8]. The antenna elements are orthogonally oriented to each other with spacing of $0.3\lambda_0$ between elements, including electromagnetic bandgap (EBG) structure, defected ground structure (DGS), capacitive elements (CE), and neutralisation line (NL), to increase isolation between the MIMO antenna elements with low complexity and cost. A compact size MIMO amer fractal slot antenna has been proposed and energised by a CPW (coplanar waveguide) to control electromagnetic energy leakage for 1.5–30 GHz frequency band [9]. A low-profile, compact quad-port super-wideband (SWB) MIMO antenna was presented for internet of things (IoT) applications [10]. Four identical sickle-shaped resonating components were activated by tapered CPW feed lines in the proposed antenna. To achieve high port isolation, the antenna elements are organised in rotational symmetry (mutually orthogonal to each other). A planar, compact UWB MIMO antenna with four elements was proposed in [11], which achieved band rejection from 4.91 to 6.41 GHz. An L-C stub attached to the ground plane was used for rejection. To reject the band from 2.5 GHz to above 8.8 GHz, the length of the stub is modified.

In [12], a linearly polarised 4×4 MIMO antenna has been proposed for LTE application with an impedance bandwidth of 1.66–2.17 GHz. It combined 1800 phase reversed and phase rotated antenna elements. The proposed antenna has electrical dimension of $0.38\lambda_0 \times 0.54\lambda_0$ at a lower frequency of 1.66 GHz with isolation > 12 dB. In [13], a four-port modified rectangular radiator has been proposed for 5.7 GHz wireless application using multiple cuts and partially stepped ground. No decoupling structure is used for isolation and the proposed antenna achieved an isolation > 13 dB with an ECC of 0.04. In [14], a four-port common radiating element MIMO antenna was proposed for 2.4 GHz Wi-Fi applications. It is comprised of four radiators with partial ground planes and a diagonal parasitic element to enhance the isolation between the ports. It has an electrical dimension of $0.56\lambda_0 \times 0.56\lambda_0$ with an ECC of 0.01 and isolation > 13 dB. A 4-element wideband printed modified monopole-based MIMO antenna system was presented [15]. To improve isolation, a defective ground structure based on a combination of an array of vertical slots and one circular slot was used. The observed frequencies range from 2.017 to 2.265 GHz. In [16], a broadband printed directive antenna with parasitic strip and compact size was presented, which was designed as an antenna element for the MIMO system. A meander dipole, a concave parabolic reflector, and a parasitic strip were used to provide good impedance matching on the antenna. The suggested MIMO array provides a broad impedance bandwidth of 23.9% (0.63 GHz, 2.32–2.95 GHz) according to experimental data.

In this article, 4×4 MIMO antenna with electrical dimension $0.45\lambda_0 \times 0.45\lambda_0$ is proposed, where λ_0 represents the free-space wavelength at the lower frequency of 3.35 GHz. The operating bandwidth of the proposed antenna is 3.35–5.73 GHz by using a tapered feed along with a partial ground plane associated with rectangular stubs. The minimum and maximum isolation of the proposed antenna are 10.2 dB (3.35–3.8 GHz) and 27 dB (5.5 GHz) respectively, with ECC < 0.003 , the peak gain 2.74 dBi, and average total efficiency of 85%. The designed antenna has a compact volume that includes four radiating elements with good diversity performance. The proposed antenna can find multiple wireless applications such as WLAN, LTE, and 5G frequency range.

2. Design

To overcome the multipath fading factors such as diffraction, reflection, and scattering due to dynamically varying wireless environment that affects the UWB/SWB antenna characteristics. The reliability, robustness, and security of the receiving system improve as the number of an antenna with identical spectral characteristics increases at the receiving terminal however, space is a major concern. Also, the effect of mutual coupling increases as the distance between antenna elements decreases, which affects the diversity performance of the MIMO system.

2.1. Single element

The geometry of the suggested monopole radiator antenna, which is used for the MIMO configuration, is shown in Figure 1(a, b). The monopole I-shaped radiator antenna is made of FR4 material, which has a dielectric constant of 4.4, loss tangent of 0.02, and a total volume of $24 \times 22 \times 1.6 \text{ mm}^3$. The optimised antenna parameters are listed in Table 1. The monopole antenna achieves an FBW of 30.48% (4.06–5.52 GHz) with a centre frequency of 4.75 GHz as shown in Figure 1(c). To achieve a 5G frequency band, further 2×2 and 4×4 MIMO antennas are proposed.

2.2. 2×2 MIMO antennas without stub

The 2×2 MIMO antenna is shown in Figure 2(a) without the use of a rectangular stub with dimensions of $40 \times 25 \times 1.6 \text{ mm}^3$. The S11 and S12 of the proposed antenna are shown in Figure 2(b) and it's visible that without rectangular stub matching could not be achieved.

2.3. 2×2 MIMO antennas with stub

The 2×2 MIMO antenna is shown in Figure 3(a) and (b) by adding a rectangular stub in the partial ground plane with the dimensions of $40 \times 25 \times 1.6 \text{ mm}^3$ and the optimised antenna parameters are shown in Table 2. Figure 3(c) shows the suggested antenna's S11 and S12, and it's clear that isolation is good across the entire frequency range, albeit matching isn't quite right in the 3.4–3.8 GHz frequency band. A 4×4 MIMO antenna is proposed to cover the 3.4–3.8 GHz frequency range and enhance the channel capacity. In case of 2×2 and 4×4 MIMO antenna, the maximum channel capacity is 11.34 bits/s/Hz, and 22.68 bits/s/Hz respectively. As the number of transmitter and receiver antenna increases, the channel capacity increases without extra radiated power and spectral bandwidth.

Table 1. Single element antenna.

Symbol	Value (mm)	Symbol	Value (mm)	Symbol	Value (mm)
L_S	22	W_S	24	L_g	5
W_g	24	W_f	1.5	L_f	9
a	2	b	4	$c = d$	0.5

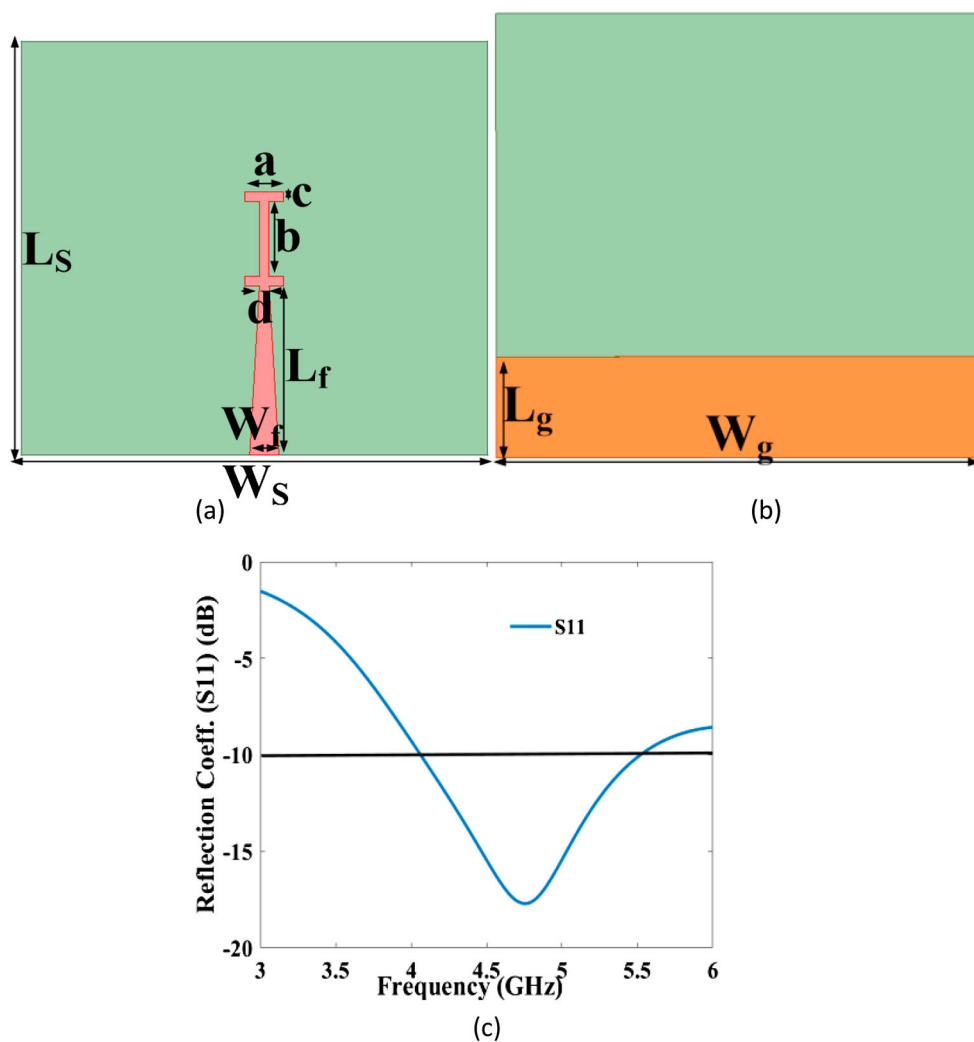


Figure 1. Single element antenna: (a) front view, (b) back view and (c) reflection Coeff.

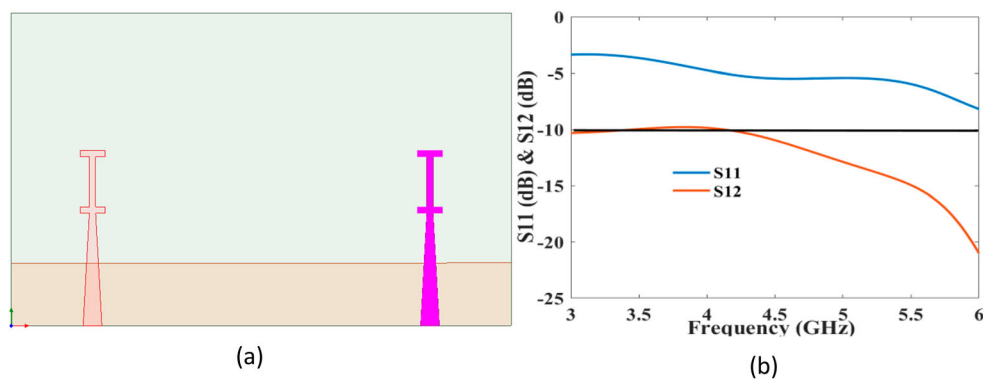


Figure 2. MIMO antenna without stub: (a) 2×2 and (b) S11 & S12.

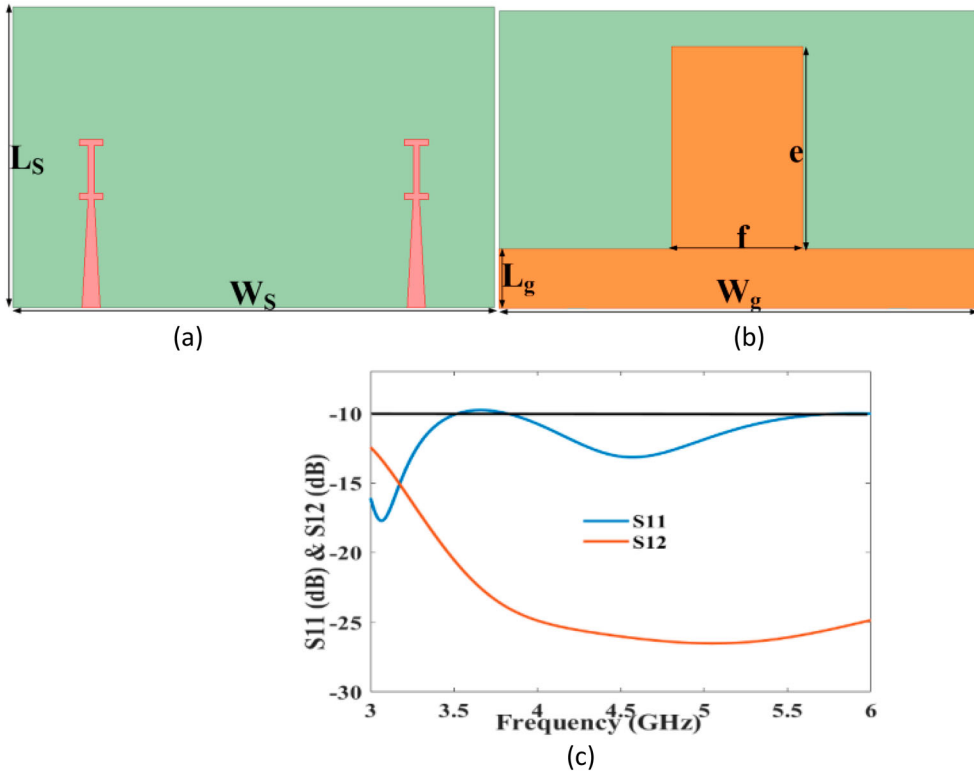


Figure 3. Dual-element MIMO antenna with stub: (a) front view, (b) back view, (c) S11 and S12.

Table 2. Dual element MIMO antenna.

Symbol	Value (mm)	Symbol	Value (mm)	Symbol	Value (mm)
L_s	25	W_s	40	L_g	5
W_g	40	W_f	1.5	L_f	9
a	2	b	4	$c = d$	0.5
e	17	f	11		

The basic building block of the proposed quad element MIMO consists of four I shaped radiators, partial ground plane associated with rectangular stubs, and tapered feed as appears in Figure 4, which has a substrate dimension of $40 \times 40 \times 1.6 \text{ mm}^3$ and is fabricated on FR4 substrate having a dielectric constant of 4.4, loss tangent of 0.02 and the optimised antenna parameters are shown in Table 3. In this case, each element is mutually coupled with the others (three resonating elements) and matching can be improved by incorporating rectangular stub in the ground plane, which acts as open circuit stub and its dimension are tuned properly to compensate for the input impedance offered by the antenna as the inductance and capacitance value depends on it. Thus desired bandwidth of the proposed MIMO antenna can be achieved by altering the dimension (e & f) of the stub.

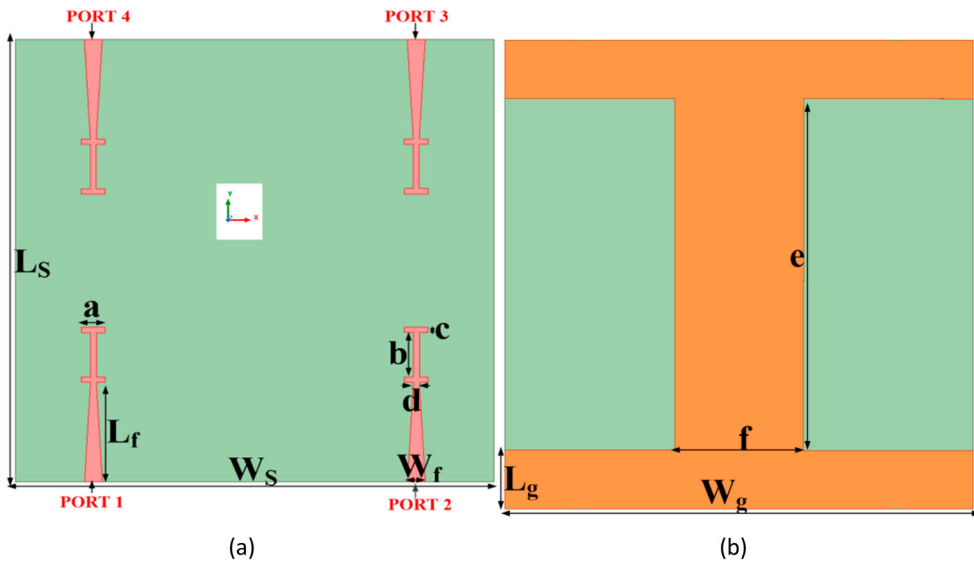


Figure 4. Proposed MIMO antenna: (a) Front view and (b) back view.

Table 3. The optimised dimensions of the quad port MIMO antenna.

Symbol	Value (mm)	Symbol	Value (mm)	Symbol	Value (mm)
L_s	40	W_s	40	L_g	5
W_g	40	W_f	1.5	L_f	9
a	2	b	4	$c = d$	0.5
e	30	f	11		

3. Parametric analysis

The antenna performance is dependent on multiple parameters. Under this title, the impacts of a few significant parameters on S11 and S12 are studied. Parametric study of reflection coefficient (S11) is done by varying one of the design variables (nearer to its optimum value) and keeping all other parameters optimally constant. The parametric study of the proposed antenna is completed by differing ground length (L_g), feed width (W_f), spacing (d) and dimensions (length (e) and width (f)) of the rectangular stubs.

S11, S12 and S14 are analysed by altering the ground length (L_g) as shown in Figure 5(a) from 4.5–5 mm with a step size of 0.1, the optimum result is obtained at 5 mm. As can be observed, S11 is unsatisfactorily at $L_g = 4.5$ mm, and also isolation < 10 dB at some frequencies, while $L_g > 5$ mm, S11 performs well in the 5.8–6.8 GHz frequency range, but radiation efficiency $< 60\%$, that's why we have not considered frequencies greater than 6 GHz. Now, by changing the feed width (W_f) from 1.4 mm to 1.6 mm and spacing (d) from 0.4 to 0.6 mm, the optimum result is obtained at W_f

$= 1.5$ mm, and $d = 0.5$ mm as shown in Figure 5(b). Further at $d = 0.6$ mm and $W_f = 1.6$ mm, S11 performs well in the 5.8–6.8 GHz frequency range but radiation efficiency is less than 60% along with ECC more than the proposed value, that's why we haven't studied frequency range higher than 6 GHz. The effect of dimensions of the stub on S11 and

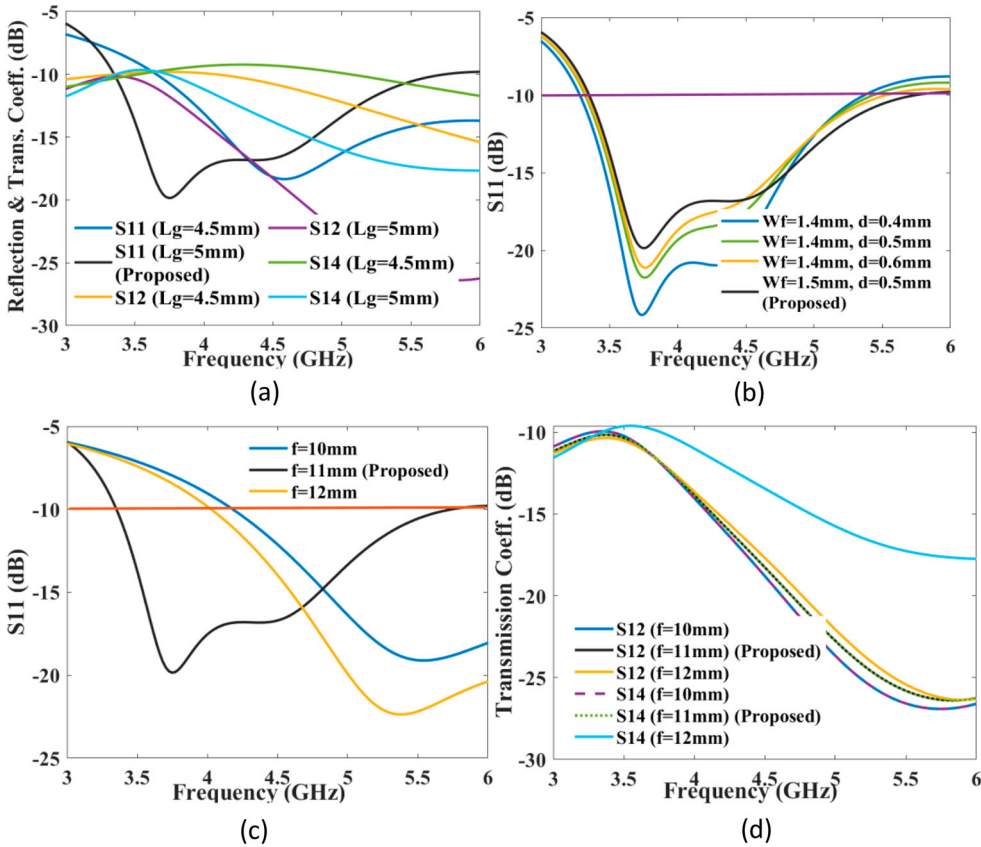


Figure 5. Parametric analysis with (a) L_g , (b) W_f and (c) stub width (S11) and (d) stub width (S12).

isolation are appeared in Figure 5(c) and Figure 5(d) respectively. The optimum bandwidth and isolation are achieved at $f = 11\text{ mm}$ and $e = 30\text{ mm}$.

Further, isolation can be improved using various techniques:

Defected ground structure (DGS). The current produced on the ground plane is coupled to the neighbouring elements, resulting in strong coupling. Mutual coupling between antenna elements can be reduced by altering the ground plane structure. The DGS or a simple ground modification plane has been introduced to provide a band-stop effect mainly by suppressing the ground current flowing between the antenna elements [17].

Decoupling network. The coupling between adjacent antennas can be reduced by using negative coupling to disconnect the adjacent antennas' input ports. Lumped components, as well as scattered elements, were employed to improve the isolation between nearby antennas. Decoupling networks (DN) have many advantages, the most important of which is their spatial efficiency [18].

Parasitic elements. The parasitic elements are not coupled to the antennas in any way. These elements are employed to provide an opposing coupling field that terminates some coupled field current between the antennas, lowering the overall coupling on the target antenna. The parasitic element generates an opposing coupling field that cancels out the original, lowering total coupling on the victim antenna [19].

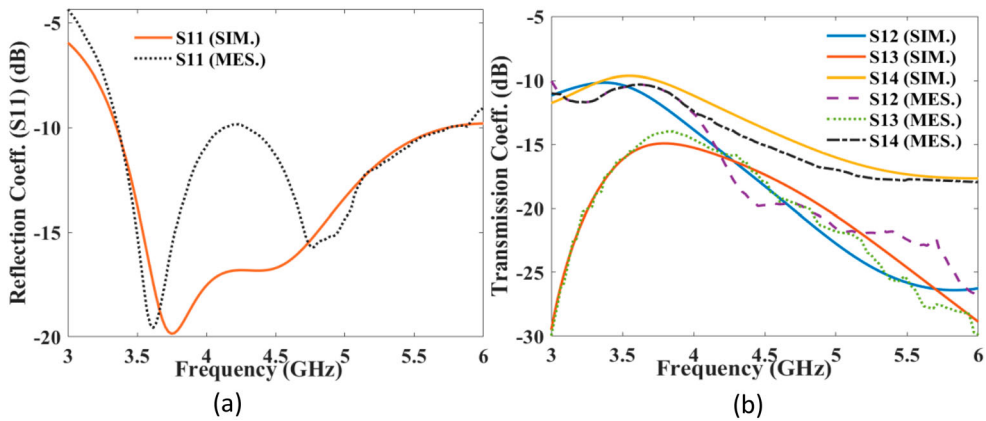


Figure 6. Simulated and measured (a) Reflection coefficient and (b) transmission coefficient.

Neutralisation lines (NL). The use of an NL helps increase the isolation between the antenna parts. The isolation can be increased with the neutralisation method because the current of the MIMO element antennas is neutralised. The current has been captured at a specific place in the input element where the impedance is lowest and the current is highest, and then its phase has been reversed by selecting a proper length for the NL. By delivering this reversed current to a nearby antenna, the coupled current can be minimised [20].

Metamaterials (MTM). Metamaterial-based antennas are divided into two categories depending on the results of the survey. MTM-based antennas and MTM inspired antennas are the two types. ENG (Epsilon Negative), MNG (μ -negative), or DNG (Double Negative) substrates are used in MTM-based antennas. The SRR (Split Ring Resonator), CSRR (Complementary Split Ring Resonator), and other MTM inspired antennas are the only ones that utilise the MTM unit cell. Single-Negative Magnetic (MNG) metamaterials are created in [21] to effectively decrease electromagnetic coupling between closely-spaced high-profile monopole antenna elements. SRR and CSRR or Capacitively-Loaded-Loops (CLL) are the most often employed MTM fundamental structures for isolation enhancement. The electromagnetic fields from the neighbouring antenna can be blocked using SRR if the external magnetic field is acting at right angles to the resonator rings [22].

4. Results and discussion

Simulated and measured, matching (S11) and isolation (S12, S13, S14) of the MIMO antenna, as represented in Figure 6 (a) and (b) are less than -10 dB, and -10 dB respectively, throughout the entire bandwidth. In the frequency range of 3.35–3.8 GHz, isolation between antenna elements 1 and 2 is approximately -10 dB, whereas antenna elements 1 and 3, and 1 and 4 are -14 dB, and -10.3 dB respectively. The average isolation between antenna elements in the 3.8–5.73 GHz frequency range is -15 dB. The discrepancy is obtained in simulated and measured results because of cable loss, tolerance and human error.

Figure 7(a) shows the peak gain of the proposed antenna at all ports. The measured peak gain of the antenna is 2.74 dBi at 4.9 GHz frequency. Figure 7(b) shows the incident,

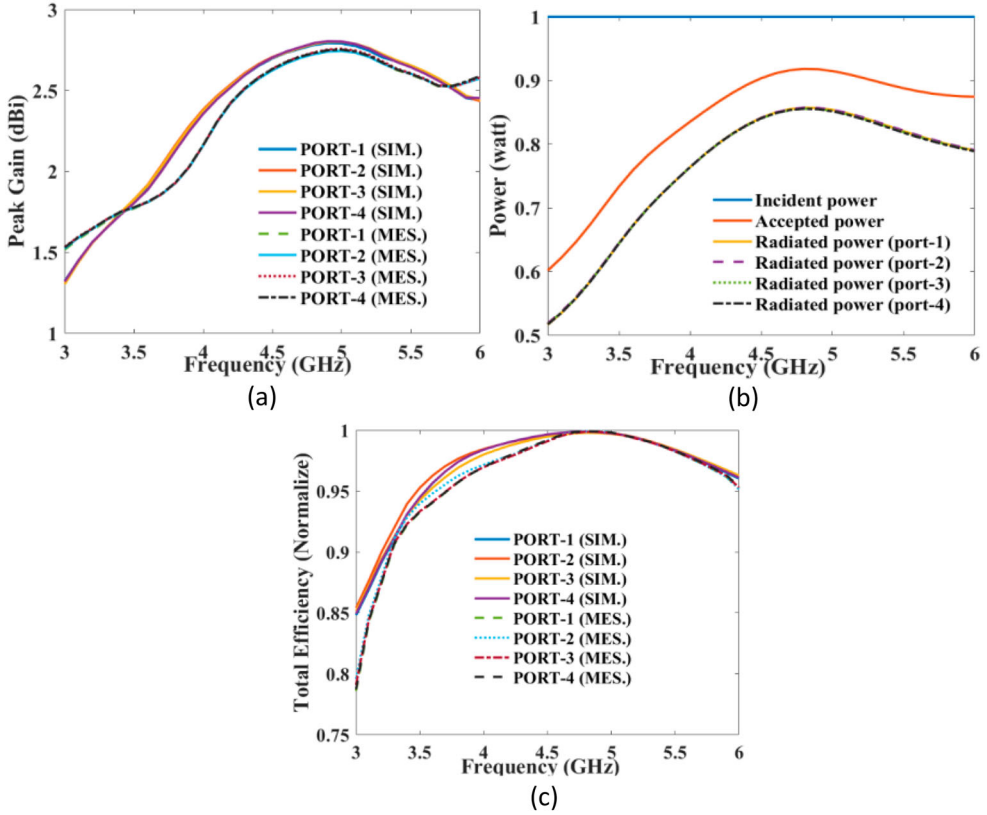


Figure 7. (a) Peak Gain, (b) power level of 4 element MIMO antenna, (c) total Efficiency.

accepted, and radiated power of the quad element MIMO antenna at all ports. Power radiated should be less than the incident and accepted power because of dielectric, conductor, and surface wave loss. Figure 7(c) represents the total efficiency at all ports of the proposed antenna. The average total efficiency is 85.1%, throughout the entire bandwidth.

Total efficiency measurement

$$n_{\text{total}}(\text{port} - 1) = n(1 - |S_{11}|^2 - |S_{21}|^2) \quad (1)$$

where η is the radiation efficiency. The radiation efficiency is defined as the ratio of the total power radiated by the antenna (P_r) to the total power accepted by the antenna (P_a) at its input terminal.

$$\eta = \frac{P_r}{P_a} \quad (2)$$

The accepted power can be calculated using

$$P_a = (1 - |\Gamma|^2)P_s \quad (3)$$

The power supplied to the antenna (P_s) can be measured using a power meter (or a receiver), and the reflection coefficient (Γ) can be measured using a vector network analyser.

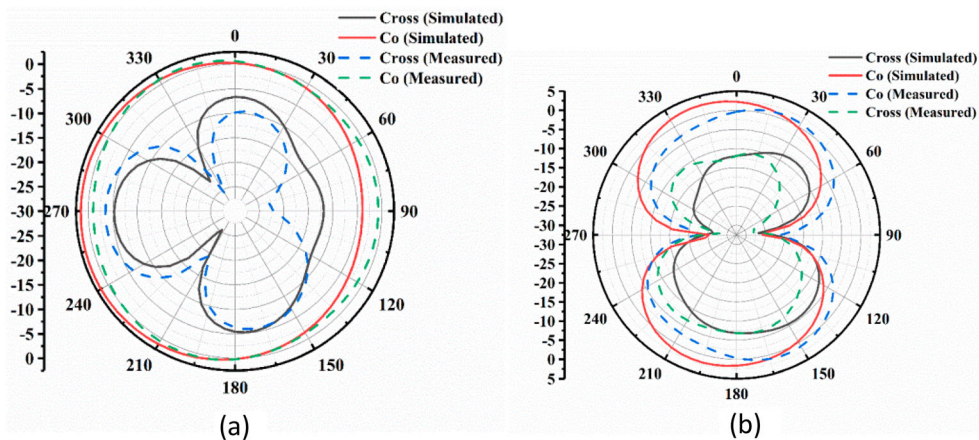


Figure 8. Co and cross polarisation: (a) YZ plane at 3.5 GHz, (b) ZX plane at 3.5 GHz.

Figure 8 represents the Co and Cross polarisation of MIMO antenna at 3.5 GHz frequency at x - z and y - z plane. The cross polar pattern is less than the co polar pattern. The co/cross-polarisation of MIMO antenna shows separation greater than -15 dB. The measured and simulated radiation patterns are in good agreement.

Figure 9 shows the surface current density of the quad element MIMO antenna at 3.5 GHz frequency. Surface currents flow in Figure 9 from the stimulated port-1 to port-4 is the fundamental reason behind the mutual coupling between close antenna elements. A low surface current is seen in other ports because of the excitation of one port and other ports terminated with a matched load. The fabricated antenna is shown in Figure 10.

5. MIMO diversity performance

The diversity characteristics of the MIMO antenna are studied in terms of ECC, TARC, MEG, DG, and CCL. The amount of correlation between the radiation patterns of MIMO elements is dictated by ECC and is determined using (4) [23].

$$|\rho_e(i, j, N)| = \frac{\sum_{n=1}^N S_{i,n}^* S_{n,j}}{\prod_{k(=i,j)} [\sum_{n=1}^N S_{i,n}^* S_{n,k}]} \quad (4)$$

Here, considered the values of $i, j, N = 1-4$ (for four elements). The value of ECC is zero for the ideal case however practical value is ≤ 0.5 . DG is portrayed as the amount of progress acquired from an array system comparative to a single element and determined as

$$DG = 10\sqrt{1 - ECC^2} \quad (5)$$

DG should be near 10 dB. The calculated values of ECC and DG are less than 0.003 and 9.98 dB respectively as depicted in Figure 11(a) and (b), which shows the good diversity performance.

In quad-port antenna, TARC is also an important parameter that gives the relation between radiated and received power. TARC can be calculated using the following equation

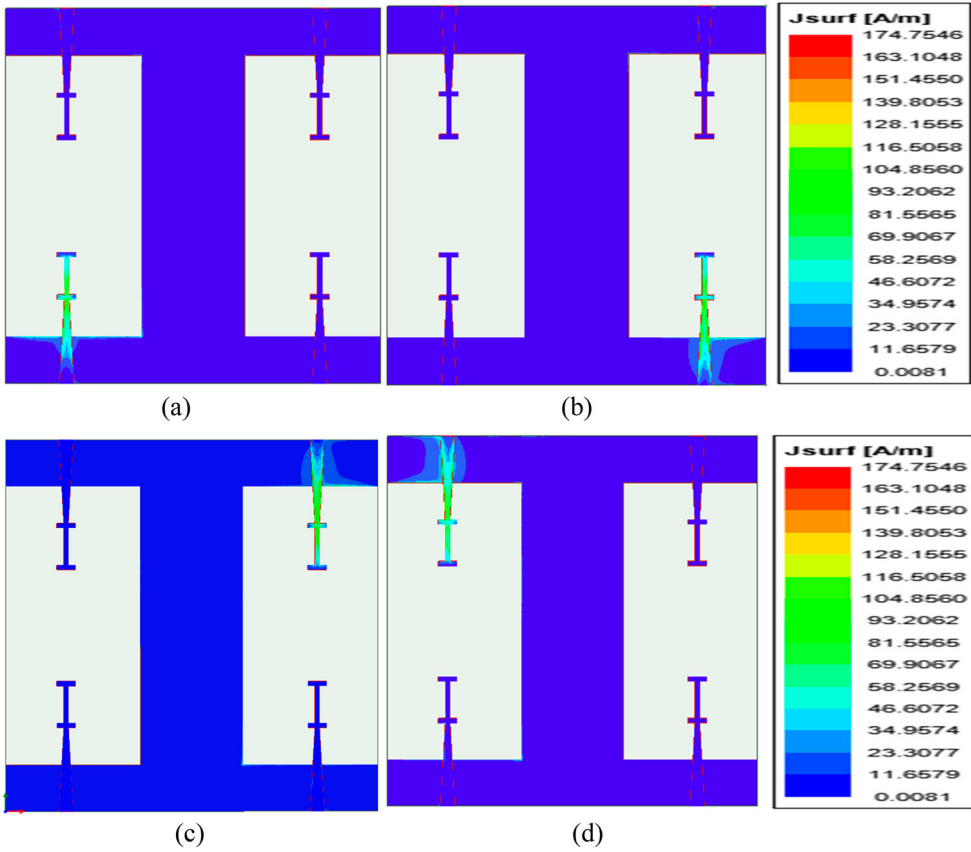


Figure 9. Surface current density at 3.5 GHz: (a) PORT-1, (b) PORT-2, (c) PORT-3, (d) PORT-4.

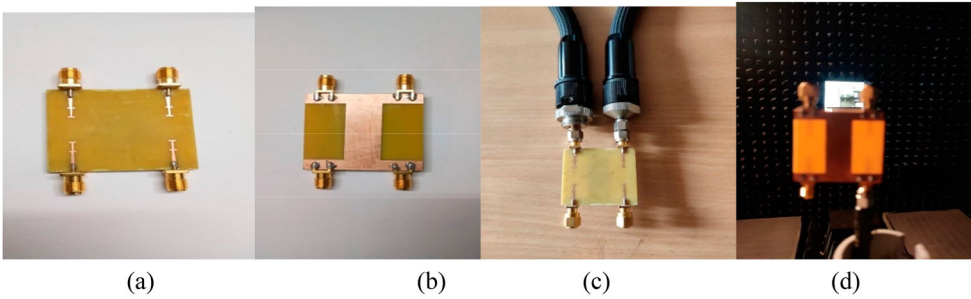


Figure 10. (a) Front view, (b) back view, (c) measurement setup of proposed MIMO antenna, (d) chamber view measurement.

[24,25]:

$$TARC = \frac{\sqrt{(|S_{ii} + S_{ij}e^{j\theta}|)^2 + (|S_{ji} + S_{jj}e^{j\theta}|)^2}}{\sqrt{N}} \tag{6}$$

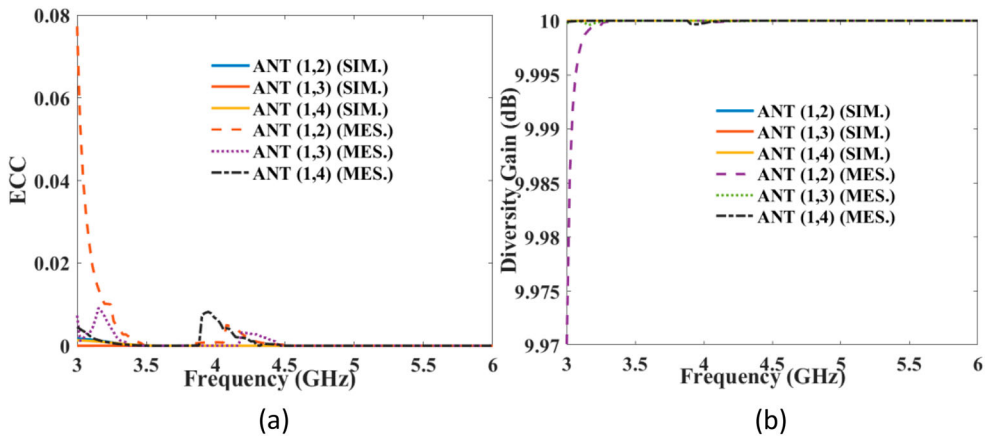


Figure 11. Simulated and Measured: (a) ECC, (b) DG.

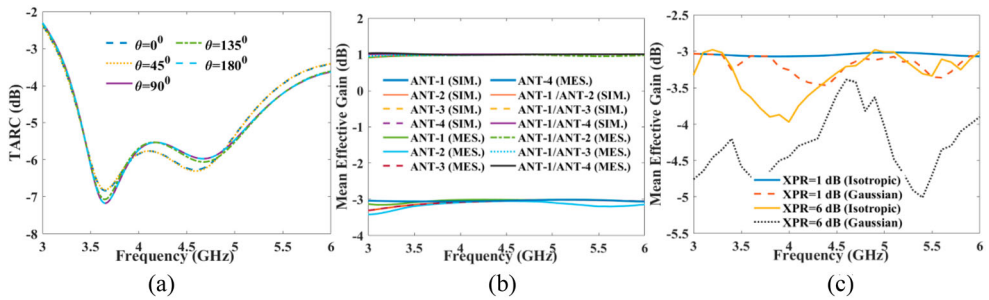


Figure 12. (a) TARC for 4×4 antenna, (b) MEG vs frequency, (c) MEG vs frequency in different medium.

where i and j are antenna elements, θ is the phase angle between any of the two adjacent/diagonal ports ranging from 0° to 180° with step increment of 45° , and N is the number of antenna/ports. In ideal case, TARC < 0 dB for MIMO antenna. The value of the TARC is less than -4 dB throughout the bandwidth as depicted in Figure 12(a).

In a fading environment, MEG is the proportion of the mean received power to the mean incident power of the antenna. The MEG is assessed for two elements using formulas (7) and (8) [26],

$$\text{MEG}_i = 0.5 \left[1 - \sum_{j=1}^N |S_{ij}|^2 \right] < -3\text{dB} \quad (7)$$

$$\text{MEG}_j = 0.5 \left[1 - \sum_{i=1}^N |S_{ij}|^2 \right] < -3\text{dB} \quad (8)$$

$$|\text{MEG}_i - \text{MEG}_j| < 3\text{dB} \quad (9)$$

$$\left| \frac{\text{MEG}_i}{\text{MEG}_j} \right| = \pm 3\text{dB} \quad (10)$$

Table 4. MEG in isotropic and Gaussian at different frequencies.

Frequency (GHz)	MEG (dB) Isotropic medium		MEG (dB) Gaussian medium	
	XPR = 1dB	XPR = 6dB	XPR = 1dB	XPR = 6dB
3.5	-3.09	-3.58	-3.20	-4.58
4.5	-3.05	-3.30	-3.34	-3.60
5.5	-3.03	-3.38	-3.35	-4.7

in which i, j denote ANT-1 and ANT-2, separately. The calculated MEG using S parameter is depicted in Figure 12(b).

The MEG is also measured using far field in outdoor (XPR = 1.0 dB) and indoor (XPR = 6.0 dB) medium as appeared in Figure 12(c) and Table 4.

$$\text{MEG}_i = \oint \left[\frac{\text{XPR} \times G_{\theta i}(\Omega) + G_{\phi i}(\Omega) \times P_{\theta}(\Omega)}{1 + \text{XPR}} \right] d\Omega \quad (11)$$

in which XPR represents the cross-polarisation ratio. The power density functions of the incident wave are $P_{\phi}(\Omega)$ and $G_{\theta i}(\Omega)$, $G_{\phi i}(\Omega)$ are the power gain, Ω represent the beam area. The value of i is 1–4 for four elements.

Channel capacity is proportional to bandwidth and signal to noise ratio (SNR). The channel capacity for four element antenna arrays is determined by (12) [27] and shown in Figure 13(a).

$$C_{4 \times 4 \text{MIMO}(\text{Max.})} = n \left(b \left[\log_2 \left[\det[I] + \frac{\text{SNR}}{n} [H][H^*] \right] \right] \right) \quad (12)$$

As the number of transmitter and receiver antenna increases, channel capacity increases, and channel capacity losses are likewise increased. CCL is calculated for two elements MIMO antenna using formula (13) [27] and shown in Figure 13(b). The practical value of CCL is less than 0.35 bits/s/Hz.

$$\text{CCL} = -\log_2 \det[\beta^R] \quad (13)$$

$$\text{where } [\beta^R] = \begin{bmatrix} \beta_{ii} & \beta_{ij} \\ \beta_{ji} & \beta_{jj} \end{bmatrix} \quad (14)$$

$$\beta_{ii} = 1 - \left(\sum_{j=1}^N |S_{ij}|^2 \right) \quad (15)$$

$$\beta_{ij} = -(S_{ii}^* S_{ij} + S_{ji}^* S_{ij}) \quad (16)$$

Table 5 compares and contrasts the diversity properties of the MIMO antenna system with previously reported articles. The MIMO antenna has a dimension of $0.45\lambda_0 \times 0.45\lambda_0$, which is compact except [9–11]. The measured value of ECC is 0.003 which is acceptable as shown in Table 5. The MIMO antenna achieves isolation between 10 and 25 dB, which is better than [11–15], but less than [8–10]. The antenna has an average total efficiency of 85% which is better than other reported antennas in Table 5, except [12]. As a result, it can be concluded that the suggested quad element MIMO antenna has favourable characteristics for use in WLAN, LTE/5G bands.

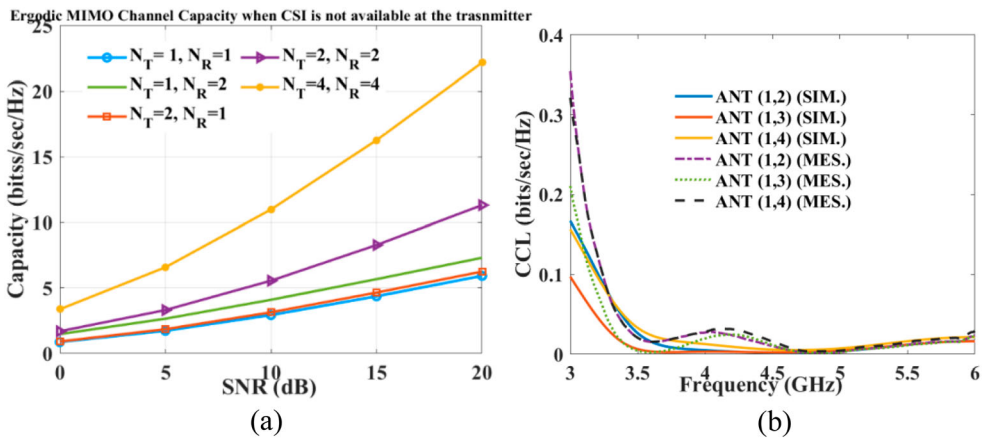


Figure 13. (a) Channel capacity of 4×4 MIMO antenna, (b) channel capacity loss (CCL).

Table 5. Comparison of proposed MIMO antenna with other proposed antenna.

Ref.	Electrical size (mm ²)	No. of ports	Frequency range (GHz)	Fractional bandwidth (FBW) (%)	Isolation (dB)	ECC
[8]	$0.50\lambda_0 \times 0.50\lambda_0$	4	3.2–5.75	56.98	20–40	0.002
[9]	$0.17\lambda_0 \times 0.17\lambda_0$	4	1.5–30	180	15–28	0.05
[10]	$0.24\lambda_0 \times 0.24\lambda_0$	4	1.3–40	187	22–32	0.03
[11]	$0.34\lambda_0 \times 0.34\lambda_0$	4	2–12 (Notch band, 4.91–6.41)	142	15–22	0.15
[12]	$0.38\lambda_0 \times 0.54\lambda_0$	4	1.66–2.17	26.63	11–18	0.23
[13]	$1.1\lambda_0 \times 1.1\lambda_0$	4	4.4–6.4	44.44	12–17	0.04
[14]	$0.56\lambda_0 \times 0.56\lambda_0$	4	2.34–2.56	8.9	10–14	0.01
[15]	$0.67\lambda_0 \times 0.4\lambda_0$	4	2.017–2.265	11.58	11	0.19
[16]	$0.68\lambda_0 \times 0.68\lambda_0$	4	2.32–2.95	23.9	17–21	0.008
This work	$0.45\lambda_0 \times 0.45\lambda_0$	4	3.35–5.73	52.42	10–27	0.003

6. Conclusion

A compact quad-element MIMO antenna of $40 \times 40 \times 1.6$ mm³ for 5G, LTE, and WLAN frequency bands is designed, fabricated, and measured. The measured results demonstrate a decent likeness to simulated ones in the whole frequency range. The proposed design's performance was evaluated and described in terms of impedance bandwidth, surface current distribution, reflection coefficient, gain, efficiency, and radiation characteristics. The MIMO provides good diversity performance with a low envelope correlation coefficient and a better diversity gain. Furthermore, within the operating frequency band, the proposed antenna obtained a maximum channel capacity of > 20 bits/s/Hz. The antenna has a total efficiency of 85.12% and a peak gain of 2.74 dBi. As a result, it is recommended as a candidate for 5G, WLAN, and LTE applications.

Disclosure statement

No potential conflict of interest was reported by the author(s).

ORCID

Ajit Kumar Singh  <http://orcid.org/0000-0001-7157-5520>

References

- [1] Agiwal M, Roy A, Saxena N. Next generation 5G wireless networks: A comprehensive survey. *IEEE Commun Surv Tutor*. 2016 Feb 19;18(3):1617–1655.
- [2] Marcus MJ. 5G and “IMT for 2020 and beyond” [Spectrum Policy and Regulatory Issues]. *IEEE Wirel Commun*. 2015 Aug 27;22(4):2–3.
- [3] Desai A, Upadhyaya T, Palandoken M, et al. Dual band transparent antenna for wireless MIMO system applications. *Microwave Opt Technol Lett*. 2019 Jul;61(7):1845–1856.
- [4] Ren Z, Zhao A. Dual-band MIMO antenna with compact self-decoupled antenna pairs for 5G mobile applications. *IEEE Access*. 2019 Jun 19;7:82288–82296.
- [5] Desai A, Bui CD, Patel J, et al. Compact wideband four element optically transparent MIMO antenna for mm-wave 5G applications. *IEEE Access*. 2020 Oct 23;8:194206–17.
- [6] Ban YL, Li C, Wu G, et al. 4G/5G multiple antennas for future multi-mode smartphone applications. *IEEE Access*. 2016 Jun 21;4:2981–2988.
- [7] Girjashankar PR, Upadhyaya T. Substrate integrated waveguide fed dual band quad elements rectangular dielectric resonator MIMO antenna for millimeter wave 5G wireless communication systems. *AEU-Int J Electron Commun*. 2021 Jul 1;137:153821.
- [8] Megahed AA, Abdelazim M, Abdelhay EH, et al. Sub-6 GHz highly isolated wideband MIMO antenna arrays. *IEEE Access*. 2022 Feb 9;10:19875–19889.
- [9] Abed AT, Jawad AM. Compact size MIMO amer fractal slot antenna for 3G, LTE (4G), WLAN, WiMAX, ISM and 5G communications. *IEEE Access*. 2019 Sep 2;7:125542–51.
- [10] Kumar P, Urooj S, Malibari A. Design and implementation of quad-element superwide band MIMO antenna for IoT applications. *IEEE Access*. 2020 Dec 17;8:226697–226704.
- [11] Khan MS, Iftikhar A, Shubair RM, et al. A four element, planar, compact UWB MIMO antenna with WLAN band rejection capabilities. *Microwave Opt Technol Lett*. 2020 Oct;62(10):3124–3131.
- [12] Malviya L, Panigrahi RK, Kartikeyan MV. Four element planar MIMO antenna design for long-term evolution operation. *IETE J Res*. 2018 May 4;64(3):367–373.
- [13] Chouhan S, Malviya L. Four-port shared rectangular radiator with defected ground for wireless application. *Int J Commun Syst*. 2020 Jun;33(9):e4356.
- [14] Chouhan S, Panda DK, Kushwah VS. Modified circular common element four-port multiple-input-multiple-output antenna using diagonal parasitic element. *Int J RF Microwave Comput-Aid Eng*. 2019 Feb;29(2):e21527.
- [15] Ikram M, Hussain R, Hammi O, et al. An L-shaped 4-element monopole MIMO antenna system with enhanced isolation for mobile applications. *Microwave Opt Technol Lett*. 2016 Nov;58(11):2587–2591.
- [16] Ding K, Gao C, Qu D, et al. Compact broadband MIMO antenna with parasitic strip. *IEEE Antennas Wirel Propag Lett*. 2017 Jun 21;16:2349–2353.
- [17] Sung YJ, Kim M, Kim YS. Harmonics reduction with defected ground structure for a microstrip patch antenna. *IEEE Antennas Wirel Propag Lett*. 2003;2:111–113.
- [18] Chen WJ, Lin HH. LTE700/WWAN MIMO antenna system integrated with decoupling structure for isolation improvement. In 2014 IEEE Antennas and Propagation Society International Symposium (APSURSI) 2014 Jul 6 (pp. 689–690). IEEE.
- [19] Ghosh S, Tran TN, Le-Ngoc T. Dual-layer EBG-based miniaturized multi-element antenna for MIMO systems. *IEEE Trans Antennas Propag*. 2014 May 13;62(8):3985–3997.
- [20] Diallo A, Luxey C, Le Thuc P, et al. Study and reduction of the mutual coupling between two mobile phone PIFAs operating in the DCS1800 and UMTS bands. *IEEE Trans Antennas Propag*. 2006 Nov 13;54(11):3063–3074.
- [21] Marqués R, Medina F, Rafii-El-Idrissi R. Role of bianisotropy in negative permeability and left-handed metamaterials. *Phys Rev B*. 2002 Apr 4;65(14):144440.
- [22] Lee JY, Kim SH, Jang JH. Reduction of mutual coupling in planar multiple antenna by using 1-D EBG and SRR structures. *IEEE Trans Antennas Propag*. 2015 Jun 18;63(9):4194–4198.

- [23] Yu K, Li Y, Liu X. Mutual coupling reduction of a MIMO antenna array using 3-D novel meta-material structures. *Appl Comput Electromag Soc J*. 2018 Jul 1;33(7):758–763.
- [24] Jaglan N, Gupta SD. Design and analysis of performance enhanced microstrip patch antenna with EBG substrate. *Int J Microwave Opt Technol*. 2015 Mar;10(2):79–88.
- [25] Glazunov AA, Molisch AF, Tufvesson F. Mean effective gain of antennas in a wireless channel. *IET Microwaves Antennas Propag*. 2009 Mar 4;3(2):214–227.
- [26] Saxena G, Jain P, Awasthi YK. High diversity gain super-wideband single band-notch MIMO antenna for multiple wireless applications. *IET Microwaves Antennas Propag*. 2020 Jan;14(1):109–119.
- [27] Singh AK, Mahto SK, Sinha R. Compact super-wideband MIMO antenna with improved isolation for wireless communications. *Frequenz*. 2021 Oct 1;75(9-10):407–417.